ASSIMILATION OF WATER VAPOR SENSITIVE INFRARED BRIGHTNESS TEMPERATURES DURING A HIGH-IMPACT WEATHER EVENT

Jason A. Otkin

Cooperative Institute for Meteorological Satellite Studies, University of Wisconsin-Madison, 1225 W. Dayton Street, Madison, WI, 53706, United States

Abstract

A regional-scale Observing System Simulation Experiment was used to examine the impact of water vapor sensitive infrared brightness temperatures on the analysis and forecast accuracy of a high impact weather event. Overall, the wind and temperature analyses at the end of the assimilation period were most accurate when brightness temperatures sensitive to water vapor in the upper troposphere were assimilated; however, the largest improvements in the cloud and moisture analyses occurred after assimilating observations sensitive to water vapor in the lower and middle troposphere. Compared to the Control case in which only conventional observations were assimilated, the more accurate analyses during the brightness temperature assimilation cases led to improved short-range precipitation forecasts. These results demonstrate that the ability of water vapor sensitive infrared brightness temperatures to improve not only the three-dimensional moisture distribution, but also the cloud, wind, and temperature fields, enhances their utility within data assimilation systems.

1 INTRODUCTION

Atmospheric water vapor (WV) exerts a strong influence on sensible weather through its effect on cloud cover and precipitation processes. Small changes in the spatial distribution of WV can have a profound impact on high-impact weather events, such as tropical cyclones, severe thunderstorms, winter storms, and heavy rainfall. Accurate forecasts of cloud cover and precipitation are more likely to occur when the spatial distribution of WV is accurately specified in datasets used to initialize numerical weather prediction models. Unfortunately, WV is highly variable in both space and time and is poorly sampled by in situ observations. Humidity profiles from radiosondes are very valuable, but are typically available only twice per day, are unevenly distributed, and have limited accuracy in the upper troposphere (Miloshevich, et al. 2006). Surface observations are available more often and with higher horizontal resolution, but do not provide information about the vertical structure of the WV distribution. The scarcity of conventional WV observations, particularly over the oceans, enhances the value of remotely sensed satellite observations that are sensitive to WV. Indeed, thermal infrared imagers and sounders onboard geosynchronous satellites are especially useful because of their high spatial and temporal resolution and large geographic coverage. In a study of the global impact of the primary WV observing systems on the accuracy of forecasts generated by the European Centre for Medium-Range Weather Forecasts model, Andersson et al. (2007) found that observations from radiosonde and surface stations were dominant over land, whereas microwave sensors had their greatest impact over the oceans and infrared sounders were most important in the upper troposphere. Better use of satellite WV observations in modern data assimilation systems has the potential to greatly improve model forecast accuracy (Fabry and Sun 2010).

Early studies obtained useful information about the WV field from infrared observations by generating derived quantities, such as vertical profiles of latent heating, dew point depression, and cloud liquid water, that were based on diagnosed cloud types. Subsequent work by Schmit et al. (2002) and Zapotocny et al. (2005) found that directly assimilating three-layer precipitable water (PWAT) retrievals from the GOES sounder over land improved model humidity and precipitation forecasts for up to 48 h. These studies also demonstrated that the higher temporal resolution of the GOES observations provided a larger forecast impact than was achieved using observations from polar orbiting sensors. More recent studies have used advanced data assimilation methods to directly assimilate WV

sensitive infrared radiances and WV profile retrievals. Li and Liu (2009) and Liu et al. (2011) found that WV retrievals from AIRS and MODIS reduced hurricane forecast intensity and track errors when assimilated using an ensemble Kalman filter (EnKF) system. Direct radiance assimilation using 3DVAR and 4DVAR systems has also been shown to improve the analysis and forecast accuracy (Kopken et al. 2004; Munro et al. 2004; Stengel et al. 2010).

In this study, a regional-scale Observing System Simulation Experiment (OSSE) is used to evaluate the potential impact of WV-sensitive infrared brightness temperatures from the Advanced Baseline Imager (ABI) on the analysis and forecast accuracy during a high-impact weather event. The ABI is a 16-band imager that will be launched onboard the GOES-R satellite in 2016 (Schmit et al. 2005). Accurate radiance measurements with high spatial and temporal resolution will provide detailed information about tropospheric WV and cloud distributions over a large geographic domain.

2. EXPERIMENTAL DESIGN

Version 3.3 of the non-hydrostatic Weather Research and Forecasting (WRF; Skamarock et al. 2005) numerical forecast model was used for this study. Ensemble data assimilation experiments were performed using the Data Assimilation Research Testbed system (Anderson et al. 2009). Temporally and spatially varying covariance inflation values were computed at each grid point using the methodology described by Anderson (2007, 2009). Sampling errors were reduced using vertical and horizontal covariance localization (Mitchell et al. 2002; Hamill et al. 2001) based on a compactly supported fifth-order correlation function. The simulated infrared brightness temperatures were assimilated using the Successive Order of Interaction (SOI) forward radiative transfer model (Heidinger et al. 2006). WRF model data used by the SOI model includes the WV mixing ratio, atmospheric and surface skin temperatures, 10-m wind speed, and the mixing ratios for each hydrometeor species predicted by the microphysics parameterization scheme.

Data from a high-resolution (6-km) “truth” simulation was used to generate simulated observations for the ABI sensor and for three conventional observing systems, including radiosondes, aircraft pilot reports, and surface reporting stations. The SOI model was used to compute simulated brightness temperatures for three ABI bands sensitive to WV in the upper troposphere (band 8; 6.19 mm), middle troposphere (band 9; 6.95 mm), and lower troposphere (band 10; 7.34 mm). These bands are also sensitive to clouds if they are located near or above the peak in the weighting function profile for a given band. For comparison to prior work by Otkin (2010, 2012), simulated brightness temperatures were also computed for the window band 11 (8.5 mm). The ABI observations were computed on the 6-km “truth” grid and were then averaged to 30 km resolution prior to assimilation. The observation errors used during the assimilation step were set to 2.5 K, 2.8 K, 3.5 K, and 5 K for bands 8, 9, 10, and 11, respectively, for both clear and cloudy observations. Larger observation errors are necessary for bands peaking lower in the troposphere since their sensitivity to a greater depth of the atmosphere can potentially result in larger representativeness errors.

3. ASSIMILATION RESULTS

The assimilation experiments begin at 06 UTC on 24 December 2009. Initial conditions valid at this time were created for a 60-member ensemble by adding initial and lateral boundary perturbations to 0.5° FNL analyses at 00 UTC on 23 December and then integrating the ensemble for 30 hours to increase the ensemble spread. The experiments were performed on a 272 x 216 grid point domain with 15-km horizontal grid spacing and 37 vertical levels. Five assimilation experiments were used to evaluate the impact of WV sensitive infrared brightness temperatures on the analysis and forecast accuracy. Simulated conventional observations were the only observations assimilated during the Control case, while both conventional observations and clear and cloudy-sky brightness temperatures were assimilated during the other cases. Observations from the ABI 6.19 mm, 6.95 mm, 7.34 mm, and 8.5 mm spectral bands were assimilated during the Band-08, Band-09, Band-10, and Band-11 cases, respectively. Simulated radiosonde observations were assimilated at 12 UTC, whereas all other observations were assimilated every 30 min during a 6-hr period from 06 UTC until 12 UTC on 24 December. The horizontal and vertical covariance localization radii were set to 600 km and 6 km,

respectively, for the conventional observations. Sensitivity tests revealed that much smaller horizontal radii were necessary for the brightness temperature observations to account for their higher spatial resolution and the potential for larger uncertainties in the representativeness of small-scale cloud and WV features detected by infrared sensors. For these observations, the horizontal localization radius was set to 100 km for band 11 and to 200 km for bands 8, 9, and 10. Vertical covariance localization was not used for the brightness temperature observations since they are sensitive to broad layers of the atmosphere. The model state vector includes the surface pressure, WV mixing ratio, temperature, horizontal and vertical wind components, and the mixing ratios for cloud water, rainwater, ice, snow, and graupel.

3.1. TIME SERIES ERROR ANALYSIS

Figure 1 shows the temporal evolution of the prior and posterior root mean square errors (RMSE) during the 6-hr assimilation period for the cloud water path (CWP) and PWAT fields. Large improvements were made to the moisture and cloud analyses during each assimilation cycle regardless of which infrared band was assimilated; however, the smallest errors tended to occur when Band-10 (7.34 mm) observations were assimilated. Given that the PWAT magnitude is strongly dependent on the moisture content in the lower troposphere, it is not surprising that the RMSE decreases as the sensitivity of the WV bands moves from the upper troposphere (Band-08) to the lower troposphere (Band-10) simply because the lower-peaking channels will have a stronger influence where most of the column WV is located. Even though Band-11 observations are not directly sensitive to moisture, their greater sensitivity to low-level clouds still led to lower PWAT errors due to the close relationship between water vapor and clouds. All of the WV band experiments exhibit lower CWP errors (Fig. 1b) than the Band-11 and Control cases, which is encouraging since this indicates that improvements made to the moisture field by water vapor sensitive infrared brightness temperatures also contribute to a more accurate cloud analysis.

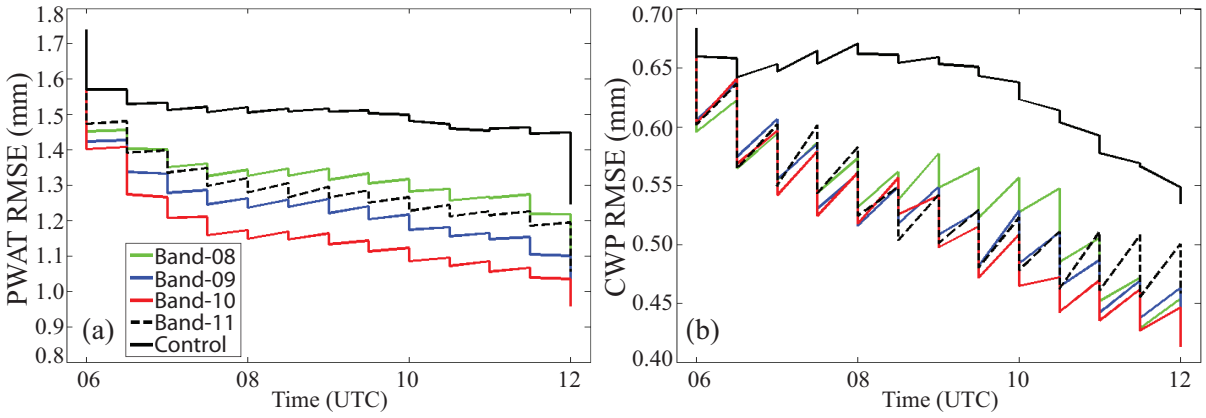

Figure 1: **Time evolution of the ensemble mean forecast and analysis (sawtooth pattern) root mean square error from 06 UTC on 24 December to 12 UTC on 24 December for (a) precipitable water (PWAT; mm), and (b) cloud water path (CWP; mm). Results are shown for the Band-08 (green), Band-09 (blue), Band-10 (red), Band-11 (dashed black) and Control (solid black) experiments.**

3.2. FINAL ANALYSIS ACCURACY

The accuracy of the final analysis at the end of assimilation period is assessed in this section. Figure 2 shows vertical profiles of RMSE for relative humidity, total cloud hydrometeor mixing ratio (QALL; sum of the cloud water, rain water, pristine ice, snow, and graupel mixing ratios), temperature, and vector wind speed. The statistics were computed using data from the posterior ensemble mean at 12 UTC on 24 December. Compared to the Control case, the relative humidity, cloud, and wind analyses were all improved during the brightness temperature assimilation cases. With the exception of the upper troposphere, the temperature analysis was also more accurate during these cases. The results show that 6.95 μm (Band-09) and 7.34 μm (Band-10) brightness temperature observations had the largest positive impact on the moisture and cloud fields, while the thermodynamic fields were most

accurate when the 6.19 μm (Band-08) brightness temperatures were assimilated. All of the WV band cases were generally more accurate than the 8.5 μm (Band-11) results and were much more accurate than when only conventional observations were assimilated during the Control case.

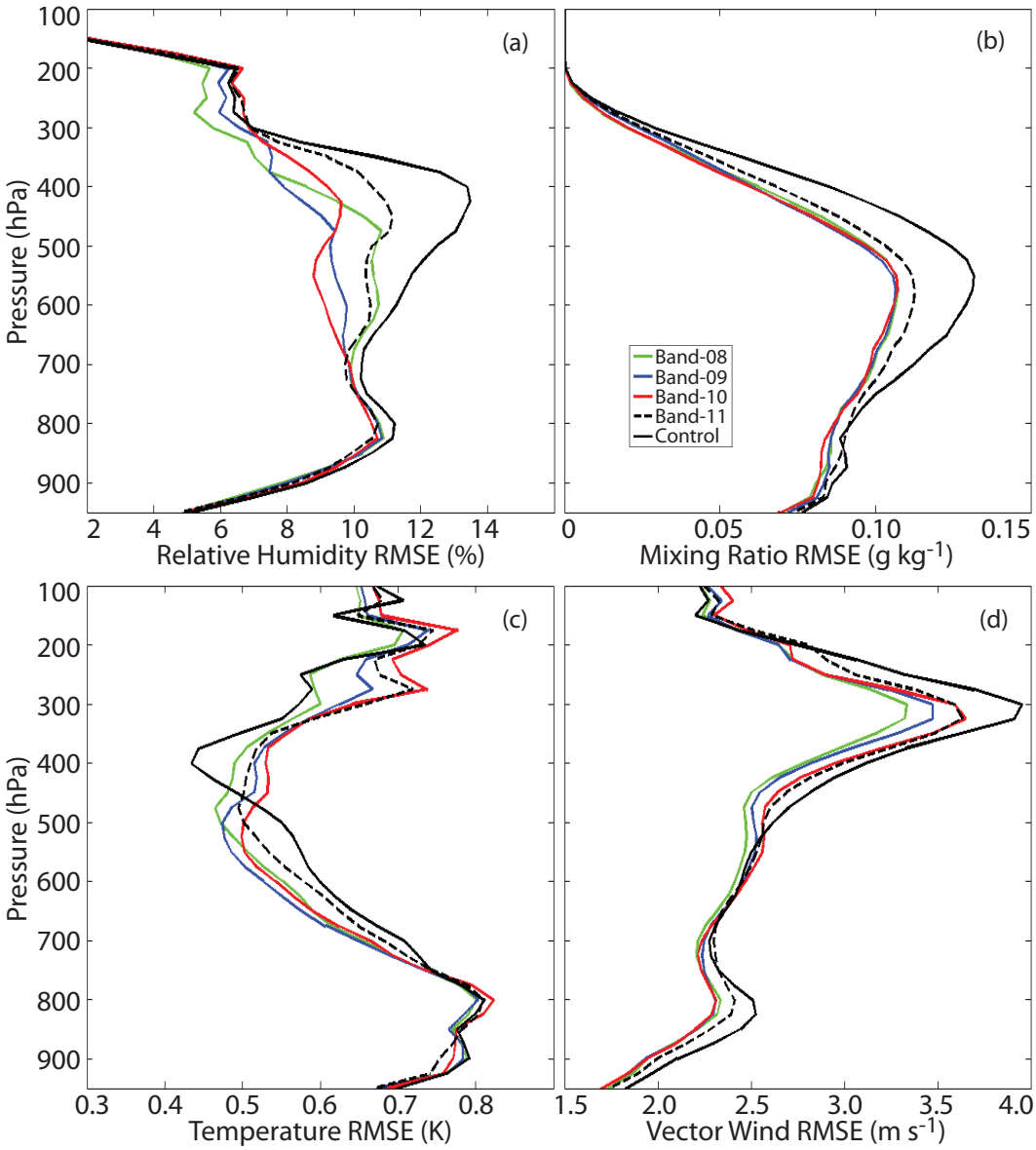

Figure 2: **Vertical profiles of root mean square error for (a) relative humidity (%), (b) total cloud hydrometeor mixing ratio (g kg^{-1}; sum of cloud water, rainwater, pristine ice, snow, and graupel), (c) temperature (K), and (d) vector wind speed (m s^{-1}). The profiles were computed using data from the posterior ensemble mean at 1200 UTC on 24 January 2009. Results are shown for the Band-08 (green), Band-09 (blue), Band-10 (red), Band-11 (dashed black) and Control (solid black) experiments.**

3.3. FORECAST IMPACT

To assess the observation impact on short-range model forecast skill during this high-impact weather event, 6-hr ensemble forecasts were performed for each case using the final ensemble analyses from 12 UTC on 24 December. Figure 3 shows the 6-hr accumulated precipitation from 12 UTC until 18 UTC on 24 December for the truth simulation and for each assimilation case. Two areas of heavier precipitation were present in the truth simulation (Fig. 3a), including a narrow band of snow extending from north central Texas to eastern Iowa, and an elongated area of very heavy rainfall associated with deep convection along the Mississippi River. During the Control case, the area of heavy rainfall along

the Mississippi River was generally well predicted; however, further to the west, precipitation amounts were too low within the region of heavy snowfall over Oklahoma and southeastern Kansas but were too high further to the north across northeastern Kansas and Iowa. The forecasts were much more accurate within this region during the water vapor band assimilation cases. This includes the location of the heaviest snowfall and its spatial orientation and also the maximum snowfall amounts. Thus, these results demonstrate that assimilation of water vapor sensitive infrared observations can reduce public risk during high impact weather events by leading to more accurate snowfall forecasts.

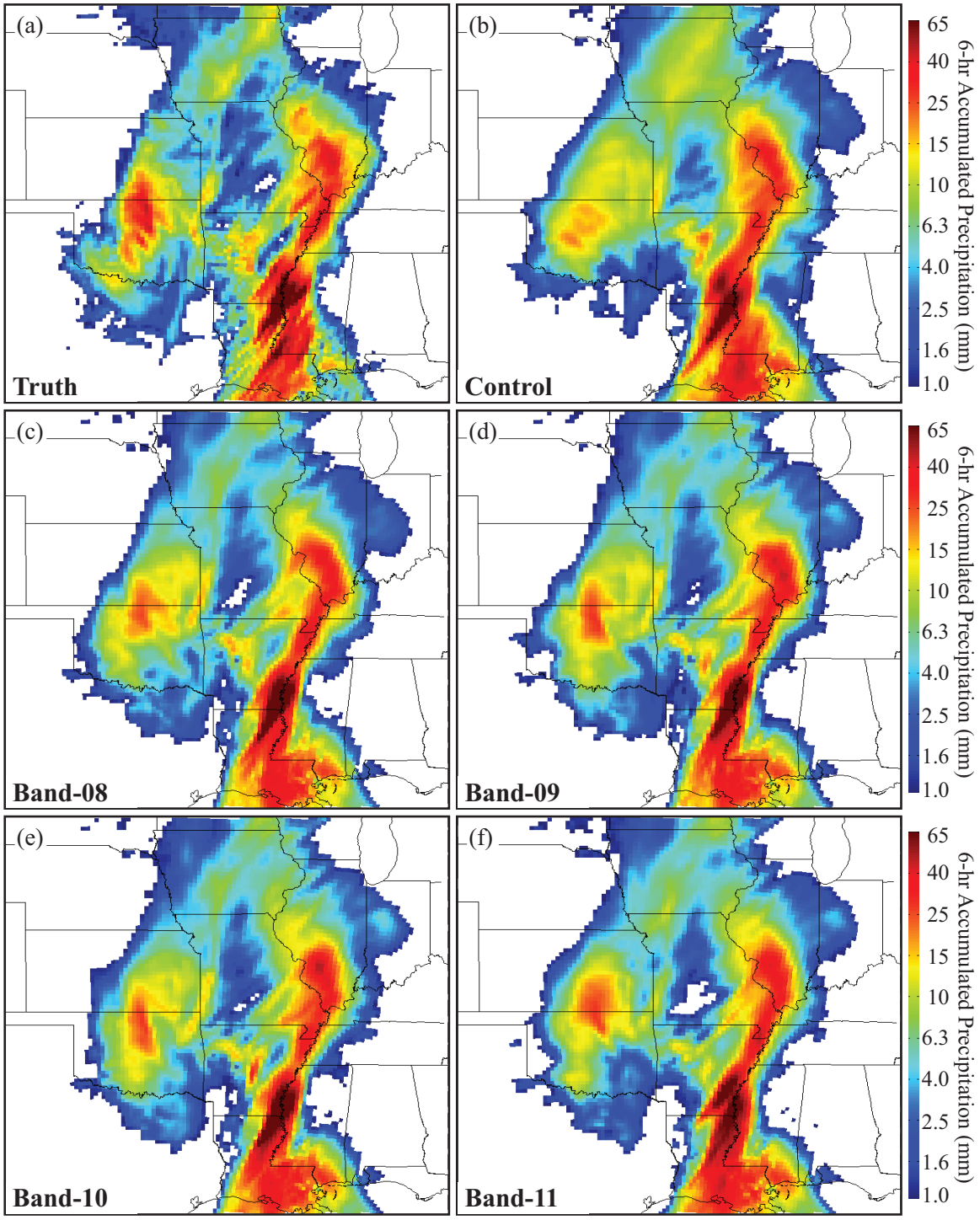

Figure 3: **Accumulated precipitation (mm) from 12 UTC until 18 UTC on 24 December for the (a) truth simulation, and for ensemble mean forecasts from the (b) Control, (c) Band-08, (d) Band-09, (e) Band-10, and (f) Band-11 experiments.**

To provide a quantitative measure of the precipitation forecast skill for each case, equitable threat scores are shown for different precipitation thresholds in Table 1. As expected, the forecast skill was consistently higher for all precipitation thresholds during the WV band assimilation cases. For the lower thresholds, the highest skill occurred during the Band-08 case; however, for heavier precipitation amounts, the skill was higher during the Band-09 and Band-10 cases. The reversal in skill scores between lower and higher precipitation thresholds during these cases may be indicative of the relative influence of the moisture and thermodynamic fields during precipitation generation processes. For instance, more accurate moisture forecasts during the Band-09 and Band-10 cases likely improved the forecast skill for heavier precipitation thresholds by modifying the amount of moisture available for cloud and precipitation development in the lower and middle troposphere. More accurate temperature and wind forecasts during the Band-08 case, however, may have exerted a stronger influence on the lighter precipitation amounts by improving the spatial coverage of the precipitation field due to a more accurate depiction of the large-scale forcing mechanisms.

	6-hr Accumulated Precipitation Thresholds (mm)				
EXP	**>0.25**	**>2.54**	**>6.35**	**>12.7**	**>25.4**
Total Events	10,749	5,946	3,152	1,599	580
Control	0.724	0.663	0.573	0.558	0.387
Band-08	**0.758**	**0.702**	0.604	0.575	0.439
Band-09	**0.756**	0.679	0.601	**0.595**	**0.450**
Band-10	0.739	0.667	**0.609**	**0.599**	0.429
Band-11	0.742	0.671	**0.608**	0.552	0.434

Table 1: **Equitable threat scores for 6-hour accumulated precipitation (mm) ending at 18 UTC on 24 December 2009. Scores are shown for precipitation thresholds > 0.25 mm, >2.54 mm, >6.35 mm, >12.7 mm, and >25.4 mm.**

4. CONCLUSIONS AND DISCUSSION

In this study, results from a regional-scale OSSE were used to examine how infrared brightness temperatures sensitive to atmospheric WV and clouds impact the analysis and forecast accuracy during a high impact weather event. Overall, the results showed that the assimilation of WV-sensitive infrared brightness temperatures had a large positive impact on both the analysis and forecast accuracy. Since the OSSE framework used during this study provides a controlled environment with an absolute measure of the true state of the atmosphere (i.e. the truth simulation), it aids and simplifies the investigation of the observation impact, but it does not fully represent an operational environment. For instance, only a small subset of the observation types assimilated at operational forecasting centers were employed during this study and no attempt was made to assimilate observations from microwave sounders or hyperspectral infrared sensors onboard polar-orbiting satellites. Although observations from these sensors have been shown to exert a positive impact on global numerical weather prediction, their utility within regional- and local-scale assimilation systems may decrease due to their much lower temporal sampling frequency. The value of geostationary sensors will increase for models with higher spatial resolution and more frequent assimilation cycles that better utilize their information content. Another important difference between this OSSE study and an operational environment is the treatment of surface emissivity over land, which can introduce significant errors for channels that are sensitive to the lower troposphere. This complication was avoided by using the same surface emissivity dataset to generate the simulated ABI observations as was used during the assimilation experiments. Since errors in the specification of surface emissivity are most important for clear sky radiance assimilation, their negative impact would have been smaller during this study even if real observations had been assimilated simply because a majority of the infrared observations were cloudy and thus not sensitive to the surface characteristics.

5. REFERENCES

Anderson, J. L. (2007), An adaptive covariance inflation error correction algorithm for ensemble filters. *Tellus, 59A*, 210-224.

Anderson, J. L. (2009), Spatially and temporally varying adaptive covariance inflation for ensemble filters. *Tellus, 61A*, 72-83.

Anderson, J., T. Hoar, K. Raeder, H. Liu, N. Collins, R. Torn, and A. Avellano (2009), The Data Assimilation Research Testbed: A community facility. *Bull. Am. Meteor. Soc., 90*, 1283-1296.

Andersson, E., E. Holm, P. Bauer, A. Beljaars, G. A. Kelly, A. P. McNally, A. J. Simmons, J.-N., Thepaut, and A. M. Tompkins (2007), Analysis and forecast impact of the main humidity observing systems, *Q. J. R. Meteorol. Soc., 133,* 1473-1485.

Fabry, F., and J. Sun (2010), For how long should what data be assimilated for the mesoscale forecasting of convection and why? Part I: On the propagation of initial condition errors and their implications for data assimilation, *Mon. Wea. Rev., 138,* 242.255.

Hamill, T. M., J. S. Whitaker, and C. Snyder (2001), Distance-dependent filtering of background error covariance estimates in an ensemble Kalman filter. *Mon. Wea. Rev., 129*, 2776-2790.

Heidinger, A. K., C. O'Dell, R. Bennartz, and T. Greenwald (2006), The successive-order-of-interaction radiative transfer model. Part I: Model development . *J. Appl. Meteor. Clim., 45*, 1388-1402.

Kopken, C., G. Kelly, and J.-N. Thepaut (2004), Assimilation of Meteosat radiance data within the 4D-Var system at ECMWF: Assimilation experiments and forecast impact, *Q. J. R. Meteorol. Soc., 130,* 2277-2292.

Li, J., and H. Liu (2009), Improved hurricane track and intensity forecast using single field-of-view advanced IR sounding measurements, *Geophys. Res. Lett., 36,* L11813, doi:10.1029/2009GL038285.

Liu, Y.-C., S.-H. Chen, and F.-C. Chien (2011), Impact of MODIS and AIRS total precipitable water on modifying the vertical shear and Hurricane Emily simulations, *J. Geophys. Res., 116,* D02126, doi:10.1029/2010JD014528.

Miloshevich, L.M., H. Vomel, D. N. Whiteman, B. M. Lesht, F. J. Schmidlin, and F. Russo (2006), Absolute accuracy of water vapor measurements from six operational radiosonde types launched during AWEX-G, and implications for AIRS validation. *J. Geophys. Res., 111,* D09S10, doi:10.1029/2005JD006083.

Mitchell, H. L., P. L. Houtekamer, and G. Pellerin (2002), Ensemble size, balance, and model-error representation in an ensemble Kalman filter. *Mon. Wea. Rev*., *130*, 2791-2808.

Munro, R., C. Kopken, G. Kelly, J.-N. Thepaut, and R. Sanders (2004), Assimilation of Meteosat radiance data within the 4D-Var system at ECMWF: Data quality monitoring, bias correction, and single-cycle experiments, *Q. J. R. Meteorol. Soc., 130,* 2293-2313.

Otkin, J. A. (2010), Clear and cloudy sky infrared brightness temperature assimilation using an ensemble Kalman filter. *J. Geophys. Res., 115***,** D19207, doi:10.1029/2009JD013759.

Otkin, J. A. (2012), Assessing the impact of the covariance localization radius when assimilating infrared brightness temperature observations using an ensemble Kalman filter, *Mon. Wea. Rev., 140*, 543-561.

Schmit, T. J., W. F. Feltz, W. P. Menzel, J. Jung, A. P. Noel, J. N. Heil, J. P. Nelson, and G. S. Wade (2002), Validation and use of GOES sounder moisture information. *Wea. Forecasting, 17,* 139-154.

Schmit, T. J., M. M. Gunshor, W. P. Menzel, J. J. Gurka, J. Li, and A. S. Bachmeier (2005), Introducing the next-generation Advanced Baseline Imager on GOES-R. *Bull. Amer. Meteor. Soc., 86*, 1079-1096.

Skamarock, W. C., J. B. Klemp, J. Dudhia, D. O. Gill, D. M. Barker, W. Wang, and J. G. Powers (2005), A description of the Advanced Research WRF Version 2. NCAR Tech. Note/TN-468+STR, 88 pp.

Stengel, M., M. Lindskog, P. Unden, N. Gustafsson, and R. Bennartz (2010), An extended observation operator in HIRLAM 4D-VAR for the assimilation of cloud-affected satellite radiances. *Q. J. R. Meteorol. Soc.*, *136,* 1064-1074.

Zapotocny, T. H., W. P. Menzel, J. Jung, and J. P. Nelson (2005), A four-season impact study of rawinsonde, GOES, and POES data in the Eta Data Assimilation System. Part I: The total contribution, *Wea. Forecasting, 20,* 161-177.